

# OPTICAL MODE PATTERN STUDY OF GAN BASED LEDS WITH AND WITHOUT NANOSCALE TOP GRATING

by

Greg Chavoor

Senior Project

ELECTRICAL ENGINEERING DEPARTMENT

California Polytechnic State University

San Luis Obispo

2012

## TABLE OF CONTENTS

I. Introduction .....	5
The PN junction revisited .....	5
The evolution of GaN .....	7
Disadvantages of GaN and potential solutions .....	8
II. Simulation .....	9
Simulation Software.....	9
III. Results.....	14
Conventional LED Results .....	14
Thin-Film LED Results.....	18
References.....	23

## **LIST OF TABLES**

Table I Conventional LED materials and properties .....	10
Table II $\text{Al}_x\text{Ga}_{1-x}\text{N}$ and its respective refractive indices .....	11
Table III Parameter values for the first structure without PhC .....	12
Table IV Parameter values for the second structure with a PhC .....	13

## LIST OF FIGURES

Figure 1 Example of a direct band gap emitting a photon .....	6
Figure 2 Example of an indirect band gap emitting a phonon .....	6
Figure 3 Two flow MOCVD diagram .....	7
Figure 4 Conventional LED ; a) p-GaN, b) MQWs, c) n-GaN, d) Al <sub>x</sub> Ga <sub>1-x</sub> N, e) GaN buffer, f) Sapphire .....	10
Figure 5 GaN thin film LED without photonic crystal grating.....	12
Figure 6 GaN thin film LED with a photonic crystal grating. ....	13
Figure 7 Optical confinement factor vs AlGa <sub>N</sub> substrate thickness .....	14
Figure 8 Mode [3,0] optical field vs position for AlGa <sub>N</sub> thicknesses 0, 100, 200, 300nm .....	15
Figure 9 Mode [3,0] optical field vs position for AlGa <sub>N</sub> thicknesses 400, 500, 600nm..	15
Figure 10 OCF vs mode order for different alloy compositions.....	16
Figure 11 Zoomed in version of OCF vs mode order for different alloy compositions...	16
Figure 12 OCF vs n-GaN Thickness for p-GaN = 0, 50, 100, 150, 200nm.....	17
Figure 13 Mode vs n-GaN Thickness while p-GaN changes from 0nm-200nm .....	18
Figure 14 Optical confinement factor plotted vs mode order for substrate thicknesses 300nm, 400nm, 500nm, and 600nm .....	19
Figure 15 Optical confinement factor plotted vs mode order for substrate thicknesses 700nm, 800nm, 900nm, and 1000nm .....	19
Figure 16 Optical confinement factor plotted vs mode order for substrate thicknesses 2000nm, 3000nm, and 4000nm .....	20
Figure 17 Optical field vs y-direction for mode [9,0]; grating periods 100nm, 230nm, and 460nm .....	21
Figure 18 Optical field vs y-direction for mode [9,0]; grating periods 690nm, 920nm, 1500nm, 2000nm, and 3000nm .....	21

## **I. Introduction**

Gallium Nitride (GaN) based semiconductors continue to prove themselves increasingly useful in the world of electronics. This not so simple III-V based semiconductor has revolutionized solid state lighting<sup>1</sup>, optical communications<sup>2</sup>, and power electronics<sup>3</sup>.

### *The PN junction revisited*

Several factors make GaN a good semiconductor for light emitting devices, the first being its direct band gap properties. The Fermi level of a semiconductor lies in between the conduction band and valence band. When temperature equals 0 Kelvin, no electrons occupy energy states above the Fermi level. As temperature increases, electrons gain energy and jump to the conduction band. Since electrons want to be in the lowest state possible, they often jump back down to the valence band and recombine with holes. As the electron moves to a lower state it releases energy in the form of light (photons) or heat (phonons). With a direct band gap, momentum does not change as the electron drops states; instead energy is released as a photon. With an indirect band gap, a change in momentum causes lattice vibrations thus releasing energy in the form of heat. Figure 1 and Figure 2 are simplified energy band diagrams that display an electron dropping from the conduction band to the valence band emitting either a photon or a phonon. The vertical direction represents electron energy (E), while the horizontal direction (K) represents momentum.

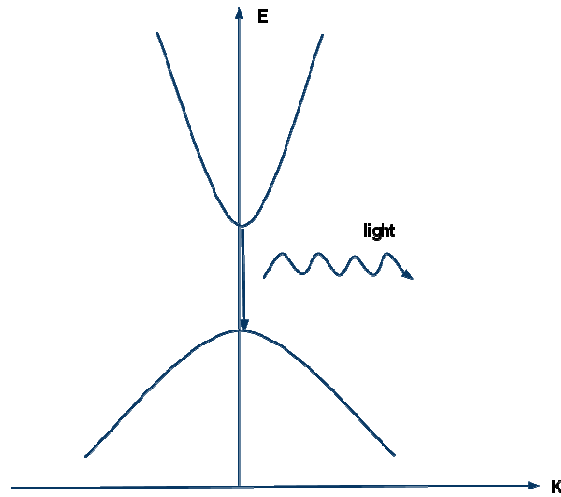


Figure 1 Example of a direct band gap emitting a photon

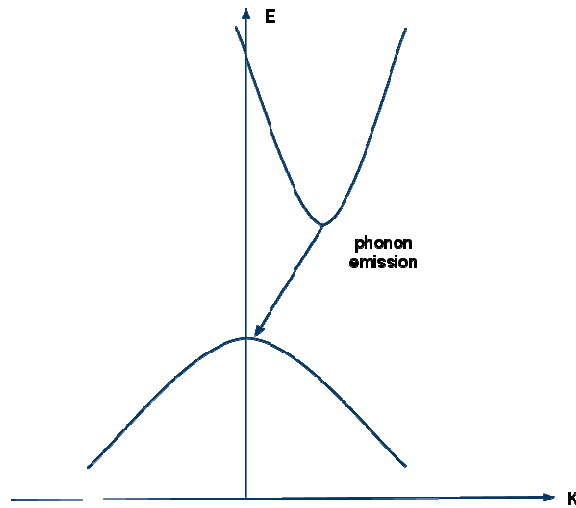


Figure 2 Example of an indirect band gap emitting a phonon

Gallium Nitride's variable band gap also makes it extremely useful for light emitting devices. For example, adjusting the composition of  $\text{In}_x\text{Ga}_{1-x}\text{N}$  can vary the band gap from 1.9eV to 3.4eV.<sup>4</sup> The equation below shows that the wavelength of light emitted depends indirectly on the energy of the gap.

$$\lambda = hc/E_g$$

Due to this relationship, a gap in the range of 1.9eV to 3.4eV will emit light in the range of yellow to blue. The values  $x$  and  $1-x$  in  $\text{In}_x\text{Ga}_{1-x}\text{N}$  represents alloy percentages. In the above case, if  $x = 0.25$  then the compound would consist of 25% Indium and 75% Ga. Changing the composition of these compound semiconductors also changes the refractive index. The new refractive index can be calculated using the following equation where the letter  $n$  represents the relative refractive indices of each material:

$$n_{\text{InGaN}} = n_{\text{InN}}x + n_{\text{GaN}}(1-x)$$

### *The evolution of GaN*

Despite GaN's advantageous properties, it also suffers from several defects such as poor crystal quality, an inability to receive p-type doping, and highly resistive p-type layers. Shuji Nakamura overcame these obstacles by producing the first high power and high luminance GaN based blue LED.<sup>5,6</sup> Nakamura implemented two techniques he developed to achieve improved crystal quality, reduced resistivity, and p-type doped GaN. The first technique was the Two Flow Metal Organic Chemical Vapor Deposition (TFMOCVD). This technique improved the lateral growth of crystals by pumping in gas perpendicular and parallel to the substrate as observed in Figure 3.<sup>7,8</sup>

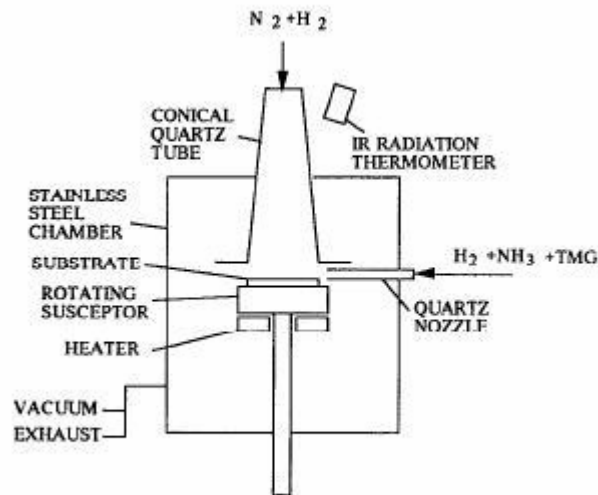


Figure 3 Two flow MOCVD diagram

The second technique he developed was annealing the substrate in a hydrogen free environment at high temperatures. This process released p-type impurities bound with

hydrogen atoms such as Mg-H and Zn-H preventing the p-type semiconductor from becoming intrinsic.

#### *Disadvantages of GaN and potential solutions*

Due to their relatively high refractive index, multiple-passive waveguides form in devices and cause transverse mode coupling. Transverse mode coupling creates ghost modes and leads to optical losses and lower device efficiencies<sup>9</sup> by decreasing the optical confinement factor. This undesirable effect often appears in GaN based laser diodes and has been previously studied.<sup>10,11,12</sup> Optical confinement factor is defined as the fraction of total mode energy that exists in the active region.<sup>13</sup> Increasing and decreasing the n-GaN or p-GaN substrate thickness alters the transverse mode patterns, and is a method used to optimize the optical confinement factor of the device<sup>14</sup>. Although these methods were primarily developed to study resonant effects in laser diodes, we use them to study the effects on conventional LEDs.

GaN's high refractive index also reduces device efficiency via total internal reflection.<sup>15</sup> Total internal reflection occurs when no light is transmitted at a boundary. The critical angle determines the angle above which light is totally reflected back and depends on the refractive index of the two mediums. Photonic crystal (PhC) gratings provide more angles for light to escape the LED and thus improve extraction efficiency. Both computer simulations and experimental data show that PhC gratings improve light extraction efficiency;<sup>16,17,18</sup> however they do not analyze how the gratings affect the optical confinement factor (OCF) and transverse mode patterns.



## II. Simulation

### *Simulation Software*

For this study, our primary goal is to understand how the thickness of each layer in a GaN based LED affects the transverse mode coupling and optical confinement factor of the device. We achieve this goal by using optical mode calculations in RSOFT's Lasermod software. The software iterates the Helmholtz equation to find the strength and location of each mode of propagation. The Helmholtz equation, defined in equation 1, allows us to determine the optical confinement factor by comparing the energy of a mode with the energy in the active region.

$$\left[ \frac{\partial^2}{\partial x^2} + \frac{\partial^2}{\partial y^2} + k_o^2 (\epsilon(x, y) - n_{eff,m}^2) \right] E_m(x, y, z) = 0$$

This equation uses the propagating field  $E_m(x, y, z)$ , refractive index  $n_{eff,m}$ , dielectric constant  $\epsilon(x, y)$ , and the propagation factor  $k_o$  to calculate the optical confinement factor. The refractive index, dielectric constant, and propagation factor are all user defined from the materials file.

### *LED LaserMOD Design*

This study focuses on maximizing optical confinement factor and reducing ghost mode effects in two GaN LED structures, a conventional LED and a thin film LED. The conventional LED consists of several layers including: p-type GaN, InGaN/GaN MQWs, n-type GaN,  $Al_xGa_{1-x}N$ , and a GaN buffer grown on sapphire. GaN is often grown on sapphire using vapor deposition techniques. The GaN buffer layer improves the crystallinity and surface morphology of the structure, a necessary step in forming p-type GaN.

First, we simulated the conventional LED. The conventional LED structure, shown in Figure 4 consists of several layers including: p-type GaN, InGaN/GaN MQWs, n-type GaN,  $Al_xGa_{1-x}N$ , and a GaN buffer grown on sapphire. Table I describes the material properties and dimensions of each of these layers. It includes the material, refractive index, substrate thickness, and doping levels.



Figure 4 Conventional LED ; a) p-GaN, b) MQWs, c) n-GaN, d)  $\text{Al}_x\text{Ga}_{1-x}\text{N}$ , e) GaN buffer, f) Sapphire

Table I Conventional LED materials and properties

Material	Refractive Index	Thickness (nm)	Doping ( $\text{cm}^{-3}$ )
p-GaN	2.5	200	$1\text{E}+17$
InGaN/GaN MQWs	2.6	50	0
n-GaN	2.5	200	$2\text{E}+18$
$\text{Al}_x\text{Ga}_{1-x}\text{N}$	varies	Varies	0
GaN buffer	2.5	3000	0
Sapphire	1.78	4000	0

In the first set of simulations we increased the thickness of  $\text{Al}_{0.1}\text{Ga}_{0.9}\text{N}$  from 0nm to 600nm in steps of 100nm. For each thickness, modal simulations inspected the optical field distribution and optical confinement factor for the first twenty transverse electric modes. In the second set of simulations we changed the x composition in  $\text{Al}_x\text{Ga}_{1-x}\text{N}$  from 0.05 to 0.2 in steps of 0.05 and calculated the existing mode's energy distribution and optical confinement factor.

**Table II** shows that adjusting the x composition in  $\text{Al}_x\text{Ga}_{1-x}\text{N}$  also affects the refractive index of the material. For these simulations, the thickness of  $\text{Al}_x\text{Ga}_{1-x}\text{N}$  remained 600nm.

Table II  $\text{Al}_x\text{Ga}_{1-x}\text{N}$  and its respective refractive indices.

Material	Refractive Index
$\text{Al}_{0.05}\text{Ga}_{0.95}\text{N}$	2.45
$\text{Al}_{0.1}\text{Ga}_{0.9}\text{N}$	2.43
$\text{Al}_{0.15}\text{Ga}_{0.85}\text{N}$	2.4
$\text{Al}_{0.2}\text{Ga}_{0.8}\text{N}$	2.38

Finally, we adjusted the p-GaN and n-GaN thicknesses in order to inspect the effect of the position of  $\text{Al}_x\text{Ga}_{1-x}\text{N}$ . Both n-GaN and p-GaN substrates were altered from 0 to 200nm in steps of 50nm resulting in a total of 25 simulations. For each iteration, one of the substrate thicknesses was held constant while the other thickness varied from 0 to 100nm. For example, in the first five simulations the n-GaN layer remained 0nm while the p-GaN layer changed from 0-200nm. For the next five simulations the n-GaN layer remained 50nm while the p-GaN layer changed from 0-200nm.

The second design is a thin film GaN based LED. Simulations were performed on two variations of the thin film LED. The first variation did not contain a photonic crystal (2PhC) grating while the second variation did. Gallium Nitride has high refractive index that leads to poor light extraction efficiencies. 2PhC gratings provide a larger critical angle and are often implemented in LED structures to improve these efficiencies.<sup>19</sup> Since crystal gratings are commonly found in thin film devices, we thought it important to analyze the effects on the transverse mode patterns and optical confinement factor.

Next we simulated a thin-film LED structure with and without a photonic crystal grating. Figure 5 displays the thin-film LED without a photonic crystal grating.

Table III includes a description of the material, refractive index, thickness, and doping for each layer. In these simulations, we altered the n-GaN substrate thickness from 300-1000nm in steps of 100nm and 1000-4000nm in steps of 1000nm. Modal analysis

investigates how changing this substrate width affects the transverse mode coupling and optical confinement factor of the device.

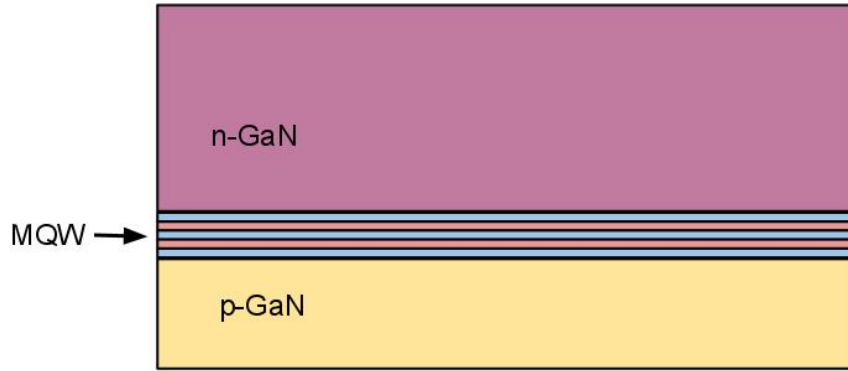


Figure 5 GaN thin film LED without photonic crystal grating.

Table III Parameter values for the first structure without PhC

Material	Refractive Index	Thickness (nm)	Doping ( $\text{cm}^{-3}$ )
n-GaN	2.5	300-1000 1000-4000	$2\text{E}+18$
InGaN/GaN MQWs	2.6	50	0
p-GaN	2.5	200	$1\text{E}+17$

Figure 6 shows the thin-film LED structure with a 2PhC grating. Table IV provides the same parameter values included in

Table III. For this structure, we performed eight simulations, each with a different grating period (100nm, 230nm, 460nm, 690nm, 920nm, 1500nm, 2000nm, 3000nm). Analysis of the optical field plots and optical confinement factor revealed the effects of the PhC grating on transverse mode coupling.

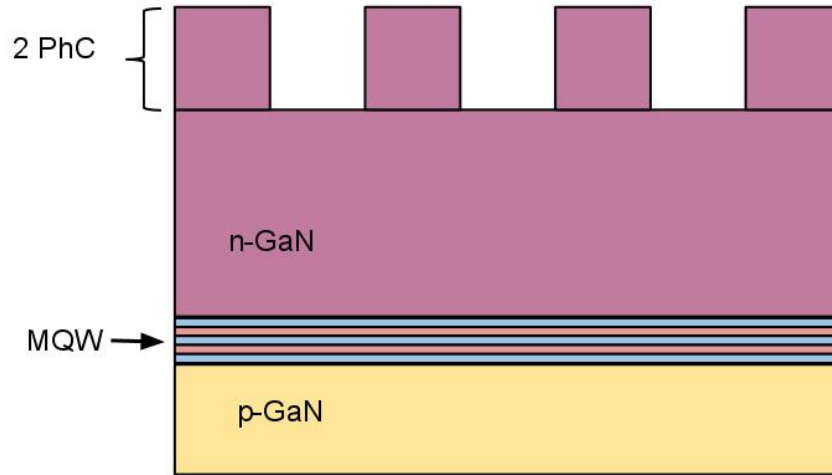


Figure 6 GaN thin film LED with a photonic crystal grating.

Table IV Parameter values for the second structure with a PhC

Material	Refractive Index	Thickness (nm)	Doping (cm <sup>-3</sup> )
n-GaN	2.5	200nm (PhC) 400nm	2E+18
InGaN/GaN MQWs	2.6	50	0
p-GaN	2.5	200	1E+17

### III. Results

#### *Conventional LED Results*

The results from the first simulation show that changing the thickness of AlGaIn profoundly affects both the optical field distribution and optical confinement factor. Figure 7 displays that as the thickness of AlGaIn increases the optical confinement factor of mode [3,0] increases and the optical confinement factor of all other modes decrease. In other words, when AlGaIn thickness is less than 300nm the ghost modes in the passive waveguide region consume a significant amount of energy and when AlGaIn thickness is greater than 300nm the active region consumes most of the energy. This effect can be observed graphically in Figure 8 and Figure 9. Figure 8 shows the optical field distribution for mode [3,0] when AlGaIn thickness is 0, 100, 200, and 300nm. Figure 9 shows the optical field distribution for mode [3,0] when AlGaIn thickness is 400, 500, and 600nm. The spikes occur in the active region at 5 $\mu$ m. The humps that occur to the left are unwanted ghost modes in the passive waveguide region.

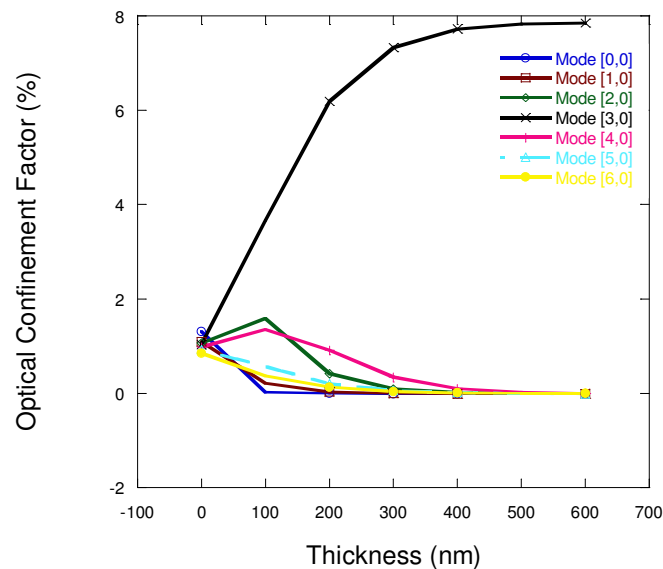


Figure 7 Optical confinement factor vs AlGaIn substrate thickness

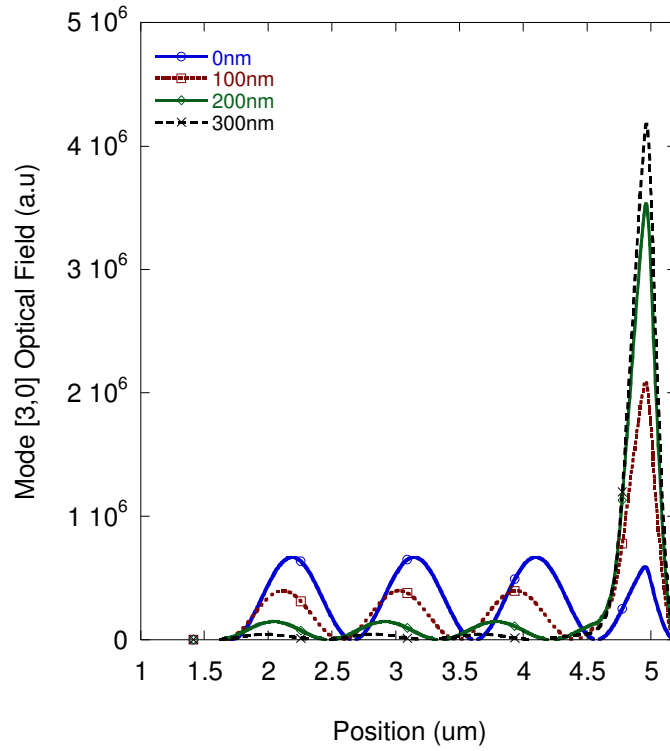


Figure 8 Mode [3,0] optical field vs position for AlGaIn thicknesses 0, 100, 200, 300nm

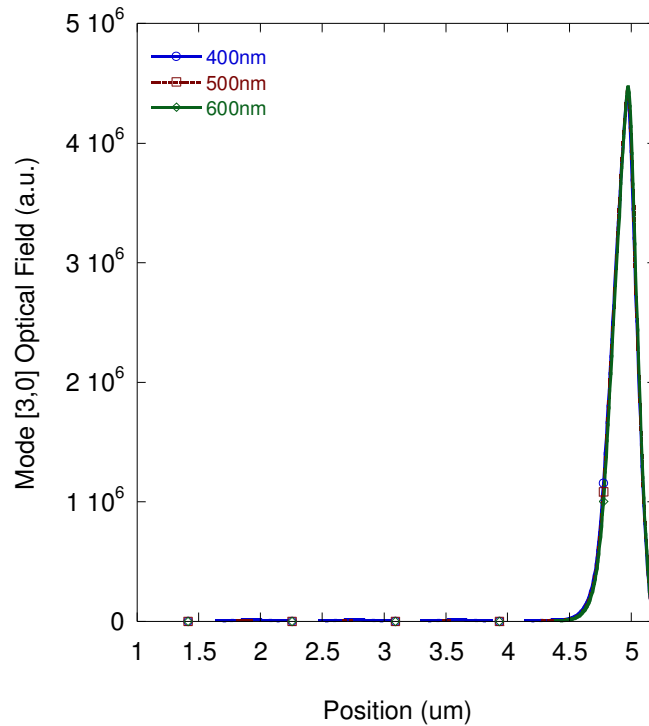


Figure 9 Mode [3,0] optical field vs position for AlGaIn thicknesses 400, 500, 600nm

The results from the second simulation show that changing the alloy composition of  $\text{Al}_x\text{Ga}_{1-x}\text{N}$  affects the optical confinement factor. Increasing the x composition from 0.05

to 0.2 increased the optical confinement factor from 7.54% to 8.24%. Figure 10 shows optical confinement factor plotted vs mode order. Since the changes in optical confinement factor are small, it is difficult to see that optical confinement increases with  $x$ . Figure 11 shows a zoomed in version of this same plot to show that as  $x$  increases OCF also increases

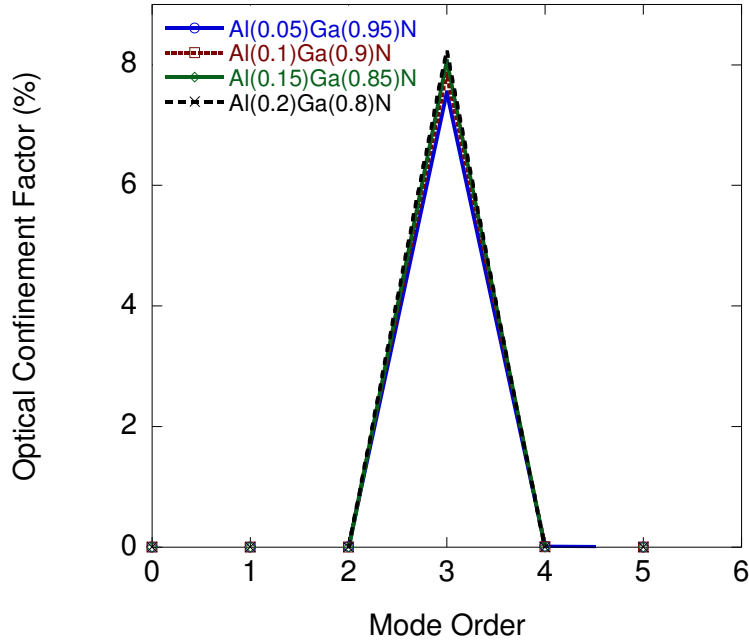


Figure 10 OCF vs mode order for different alloy compositions

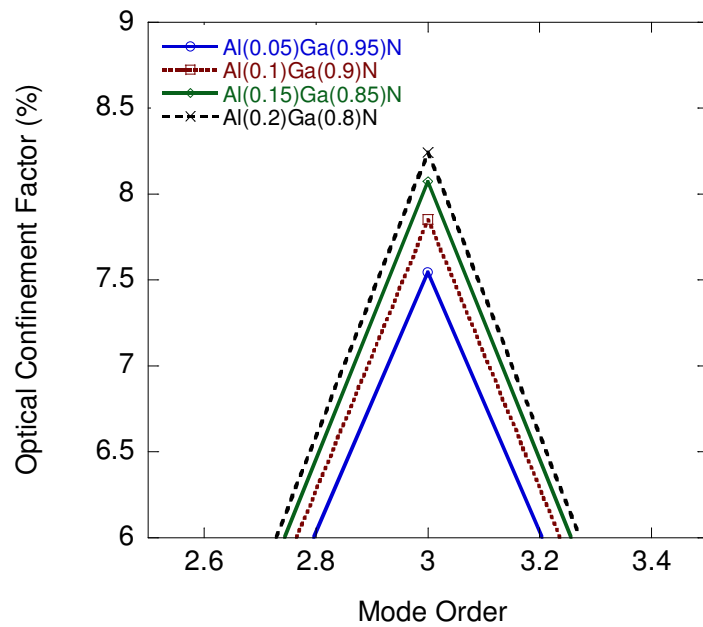


Figure 11 Zoomed in version of OCF vs mode order for different alloy compositions



The final set of simulations for the conventional LED show how the position of  $\text{Al}_x\text{Ga}_{1-x}\text{N}$  affects the optical confinement factor and light emitting mode order. Figure 12 displays that increasing the width of the p-GaN substrate generally increases the OCF. The maximum OCF occurs for p-GaN = 150nm and n-GaN = 50nm. As n-GaN increases above 50nm OCF begins to fall. Figure 13 shows that increasing p-GaN and n-GaN thickness decreases the light emitting mode order. The lowest light emitting mode order occurs when n-GaN = 200nm and p-GaN = 200nm.

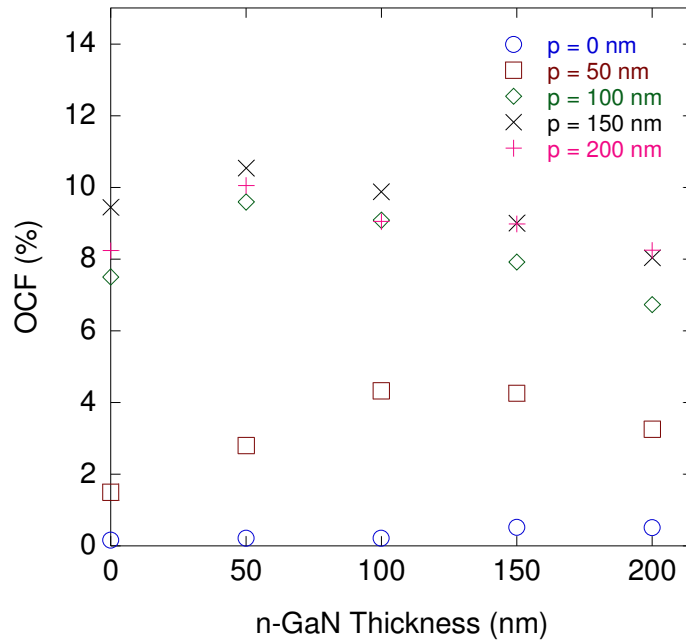


Figure 12 OCF vs n-GaN Thickness for p-GaN = 0, 50, 100, 150, 200nm

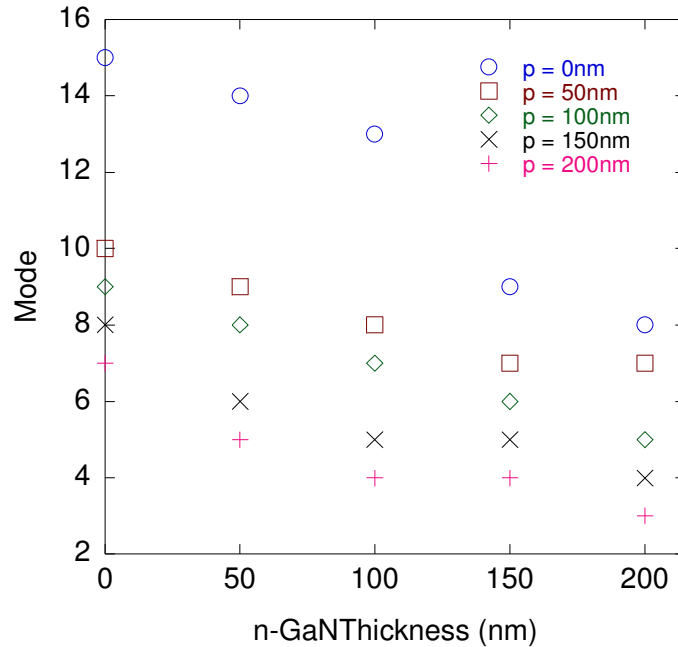


Figure 13 Mode vs n-GaN Thickness while p-GaN changes from 0nm-200nm

#### *Thin-Film LED Results*

The simulation results show that changing the n-GaN substrate thickness profoundly affected the first light emitting mode. For a substrate thickness of 300nm, the first light emitting mode occurs at mode [6,0]. Increasing the thickness to 400nm moves the first light emitting mode to mode [7,0]. All subsequent simulations follow this pattern; an increase in the substrate thickness leads to a higher order light emitting mode. Figures 9, 10, and 11 display the optical confinement factor plotted as a function of mode number for different substrate thicknesses. Optical confinement factor is defined as the fraction of total mode energy that exists in the active region [4]. Large optical confinement factors generally correspond to the light emitting mode. For the maximum substrate thickness (4000nm) in our simulation, the light emitting mode does not occur until mode [46,0]. Although the mode order increases with thickness, the maximum optical confinement factor remains constant at 46%.

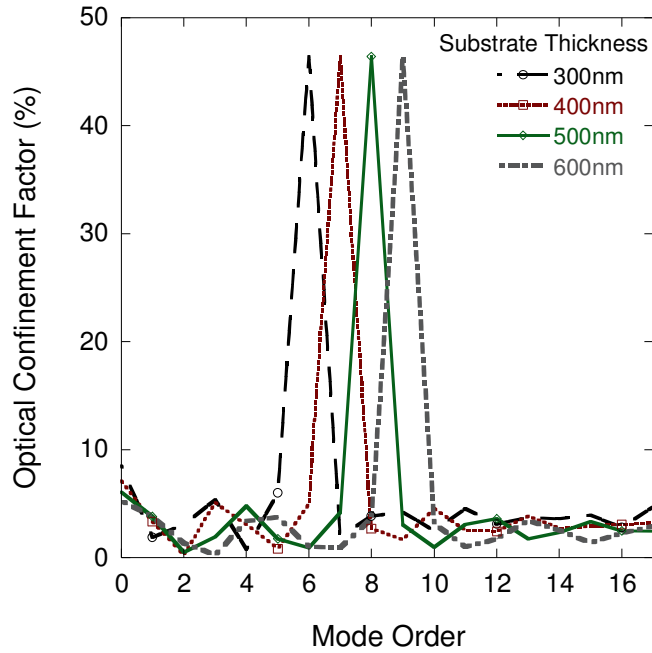


Figure 14 Optical confinement factor plotted vs mode order for substrate thicknesses 300nm, 400nm, 500nm, and 600nm

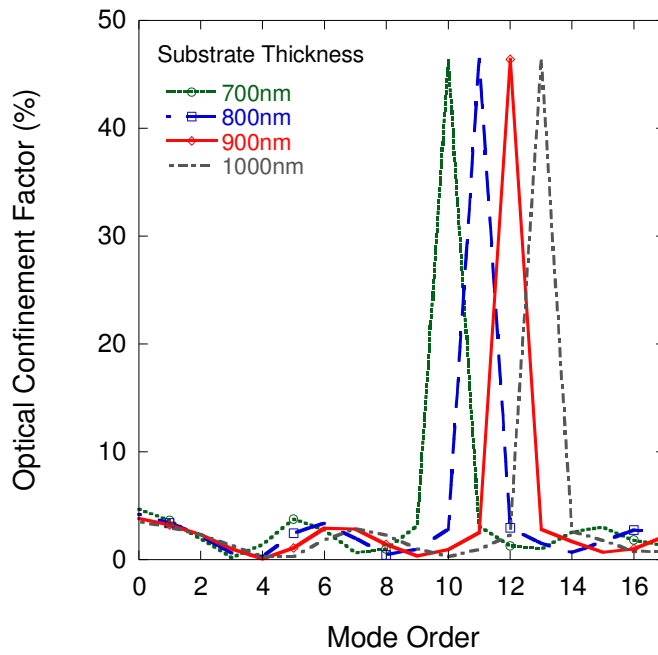


Figure 15 Optical confinement factor plotted vs mode order for substrate thicknesses 700nm, 800nm, 900nm, and 1000nm

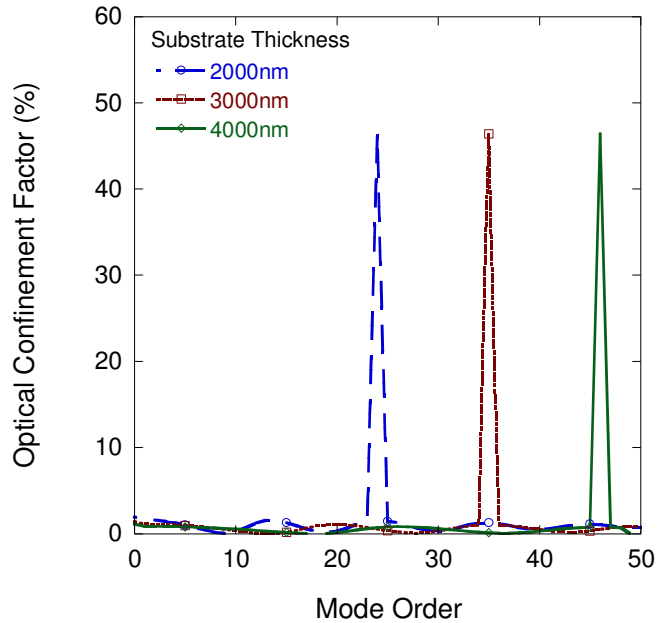


Figure 16 Optical confinement factor plotted vs mode order for substrate thicknesses 2000nm, 3000nm, and 4000nm

Unlike altering the substrate thickness, altering the grating period had no effect on the light emitting mode order. For each simulation, the light emitting mode occurred at mode [9,0] with an optical confinement factor of 46%. Although changing the grating period had no effect on optical confinement factor, it did affect the optical field intensity. Fig. 12 and Fig. 13 show that an increase in grating period corresponds to a decrease in optical field intensity. The results in Fig. 12 and Fig. 13 also show maximum optical field intensity for the 100nm structure is 5.7 times larger than the optical field intensity for the 230nm structure and 971 times larger than the optical field intensity for the 3000nm structure.

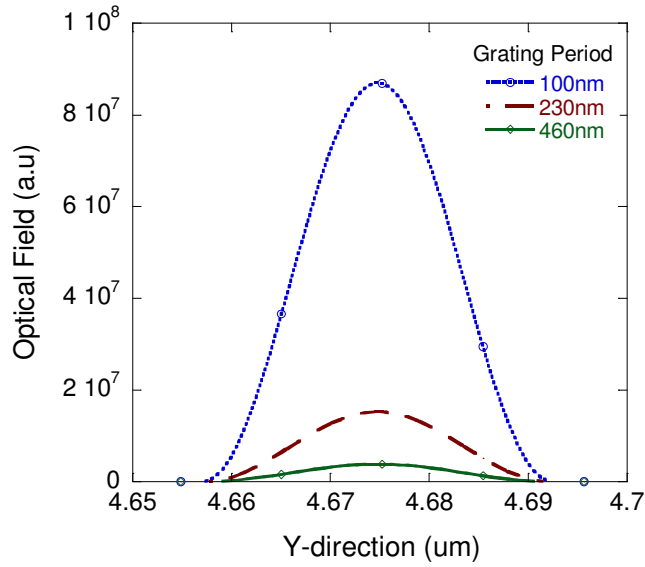


Figure 17 Optical field vs y-direction for mode [9,0]; grating periods 100nm, 230nm, and 460nm

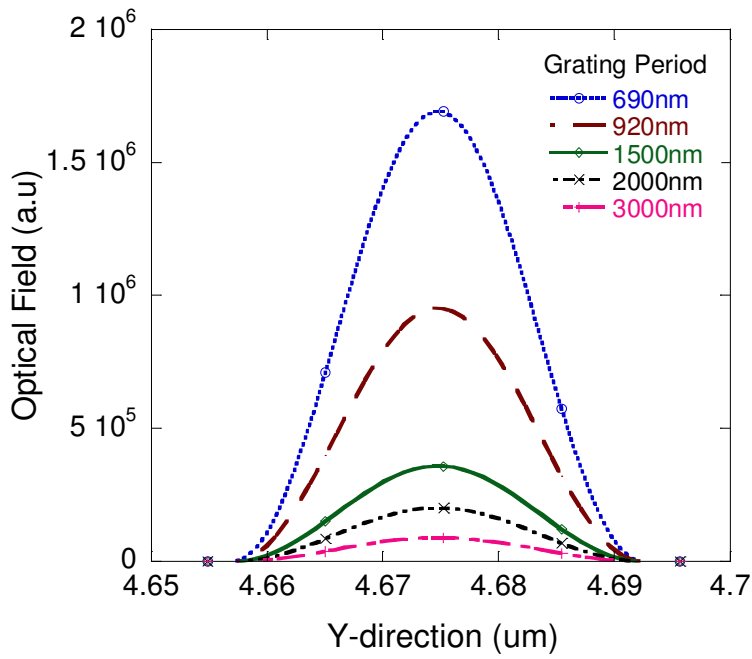


Figure 18 Optical field vs y-direction for mode [9,0]; grating periods 690nm, 920nm, 1500nm, 2000nm, and 3000nm

#### **IV. Conclusion**

Modal analysis of the three structures gives different and interesting results. Conventional LED analysis shows that optical confinement factor increases for mode [3,0] with increasing AlGaIn substrate thickness. Maximum OCF occurs when AlGaIn thickness is 600nm. We also show that increasing  $x$  from 0.05 to 0.2 in the compound  $\text{Al}_x\text{Ga}_{1-x}\text{In}$  increases OCF from 7.54% to 8.24%. Next, for the thin film LED without a PhC grating we show that increasing the n-GaN substrate thickness from 300-4000 nm increases the light emitting mode order from [6,0] to mode [46,0]. Finally the thin-film LED with a PhC grating shows that changing the grating period changes the optical field intensity but has no effect on optical confinement factor. As the grating period increases from 100nm to 3000nm the optical field decreases by a factor of almost 1000.

## References

---

- [1] Meneghini, M., Lorenzo, T., and Meneghesso, G., "A Review on the Reliability of GaN-Based LEDs," *IEEE Transactions on Device and Materials Reliability*, 8(2), 323-331 (2008).
- [2] Shaw, A.J., Bradley, A. L., Donegan, J.F., and Lunney, J.G., "GaN Resonant Cavity Light-Emitting Diodes for Plastic Optical Fiber Applications," *IEEE Photonics Technology Letters*, 16(9), 2006-2008 (2004).
- [3] Esposito, M., Chini, A., and Rajan, S., "Analytical Model for Power Switching GaN-Based HEMT Design," *IEEE Transactions on Electron Devices*, 58(5), 1456-1461 (2011).
- [4] S. Nakamura, M. Senoh, T. Mukai, "High-power InGaN/GaN double-heterostructure violet light emitting diodes," *Applied Physics Letters* 62(19), pp. 2390-2392, May 1993.
- [5] Nakamura et al., "Light-Emitting Gallium Nitride-Based Compound Semiconductor Device." US Patent 5,578,839, issued Nov. 26, 1996.
- [6] S. Nakamura, M. Senoh, T. Mukai, "High-power InGaN/GaN double-heterostructure violet light emitting diodes," *Applied Physics Letters* 62(19), pp. 2390-2392, May 1993.
- [7] Shuji Nakamura, "Crystal Growth Method for Gallium Nitride-Based Compound Semiconductor," US Patent 5,290,393, issued Mar. 1, 1994.
- [8] S. Nakamura, Y. Harada, M. Seno, "Novel metalorganic chemical vapor deposition system for GaN growth," *Appl. Phys. Lett.* 58(18), pp. 2021-2023, May 1991.
- [9] Eliseev, P.G., Smolyakov, G.A., and Osinski, M., "Ghost Modes and Resonant Effects in AlGaIn—InGaIn—GaN Lasers," *IEEE Journal of Selected Topics in Quantum Electronics*, 5 (3), 771-779 (1999).
- [10] Bougrov, V.E., Zubrilov, A.S., "Optical confinement and threshold currents in III-V nitride heterostructures: Simulation," *Journal of Applied Physics*, 81(7), 2952-2956 (1997).
- [11] Bergmann, M.J., Casey, H.C., "Optical-field calculations for lossy multiple-layer  $\text{Al}_x\text{Ga}_{1-x}\text{N}$ - $\text{In}_x\text{Ga}_{1-x}\text{N}$  laser diodes," *Journal of Applied Physics*, 84(3), 1196-1206 (1998).

- 
- [12] Mack, M.P., Young, D.K., and Abare, A.C., "Observation of Near Field Modal Emission in InGaN Multi-Quantum Well Laser Diodes by Near Field Scanning Optical Microscopy," Semiconductor Laser Conference, 9-10 (1998).
- [13] Botez, D., "Analytical Approximation of the Radiation Confinement Factor for the TE<sub>0</sub> Mode of a Double Heterojunction Laser," IEEE Journal of Quantum Electronics, 14(4), 230-232 (1978).
- [14] Jin, X., Zhang, B., Dao, T., and Zhang, G., "Effects of transverse mode coupling and optical confinement factor on gallium-nitride based laser diode," Chinese Physics B, 17 (4), 1274-1279 (2008).
- [15] Huang, X.H., Liu, J. P., and F, Y.Y., "Effect of Patterned Sapphire Substrate Shape on Light Output Power of GaN-Based LEDs," IEEE Photonics Technology Letters, 23 (14), 944-946 (2011).
- [16] Dai, T. and Zhang, B., "Light Extraction Improvement from GaN-Based Light-Emitting Diodes with Nano-Patterned Surface Using Anodic Aluminum Oxide Template," IEEE Photonics Technology Letters, 20(23), 1974-1976 (2008).
- [17] Lin, Y. Z. and Kong, F.M., "FDTD Study on the Improvement of Optical Transmission through Metallic Periodic Nano Structure," Proc. OptoElectronics and Communications Conference, 1-2 (2009).
- [18] Lee, Y. J., Kuo, H.C., and Lu, T.C., "High Light-Extraction GaN-Based Vertical LEDs With Double Diffuse Surfaces," IEEE Journal of Quantum Electronics, 42(12), 1196-1201 (2006).
- [19] S. Trieu, X. Jin, "Study of Top and Bottom Photonic Gratings on GaN LED with Error Grating Models," IEEE Journal of Quantum Electronics, 46 (10), October 2010.